Femtosecond gain and index dynamics in an InAs/InGaAsP quantum dot amplifier operating at 1.55 µm

Aaron J. Zilkie, Joachim Meier, Peter W. E. Smith, Mo Mojahedi, and J. Stewart Aitchison

Edward S. Rogers Sr. Department of Electrical and Computer Engineering, University of Toronto, 10 King's College Rd., Toronto, ON, Canada M5S 3G
aaron.zilkie@utoronto.ca

Philip J. Poole, Claudine Nì. Allen, Pedro Barrios, and Daniel Poitras

Institute for Microstructural Sciences, National Research Council Canada, Building M-50, Montreal Road Ottawa, ON, Canada K1A 0R6

Abstract: We report on the characterization of the ultrafast gain and refractive index dynamics of an InAs/InGaAsP self-assembled quantum dot semiconductor optical amplifier (SOA) operating at 1.55 µm through heterodyne pump-probe measurements with 150 fs resolution. The measurements show a 15 ps gain recovery time at a wavelength of 1560 nm, promising for ultrafast switching at >40 GHz in the important telecommunications wavelength bands. Ultrafast dynamics with 0.2-1.5 ps lifetimes were also found consistent with carrier heating and spectral hole burning. Comparing with previous reports on quantum dot SOAs at 1.1-1.3 µm wavelengths, we conclude that the carrier heating is caused by a combination of free-carrier absorption and stimulated transition processes.

OCIS codes: (320.7130) Ultrafast processes in condensed matter, including semiconductors; (999.9999) Quantum dot semiconductor amplifiers; (230.4320) Nonlinear optical devices; (250.5980) Semiconductor optical amplifiers; (070.4340) Nonlinear optical signal processing

References and Links

1. M. Sugawara, N. Hatori, M. Ishida, H. Ebe, Y. Arakawa, T. Akiyama, K. Otsubo, T. Yamamoto, and Y. Nakata, "Recent progress in self-assembled quantum-dot optical devices for optical telecommunication: temperature-insensitive 10 Gbs(-1) directly modulated lasers and 40Gbs(-1) signal-regenerative amplifiers," J. Phys. D. Appl. Phys. **38**, 2126-2134 (2005).
2. M. Sugawara, T. Akiyama, N. Hatori, Y. Nakata, H. Ebe, and H. Ishikawa, "Quantum-dot semiconductor optical amplifiers for high-bit-rate signal processing up to 160 Gb/s and a new scheme of 3R regenerators," Meas. Sci. Technol. **13**, 1683-1691 (2002).
3. T. Akiyama, N. Hatori, Y. Nakata, H. Ebe, and M. Sugawara, "Pattern-effect-free amplification and cross-gain modulation achieved by using ultrafast gain nonlinearity in quantum-dot semiconductor optical amplifiers," Phys. Status. Solidi. B **238**, 301-304 (2003).
4. A. V. Uskov, E. P. O'Reilly, R. J. Manning, R. P. Webb, D. Cotter, M. Laemmlin, N. N. Ledentsov, and D. Bimberg, "On ultrafast optical switching based on quantum-dot semiconductor optical amplifiers in nonlinear interferometers," IEEE Photonic Technol. Lett. **16**, 1265-1267 (2004).
5. P. Borri, W. Langbein, J. M. Hvam, F. Heinrichsdorff, M. H. Mao, and D. Bimberg, "Spectral hole-burning and carrier-heating dynamics in InGaAs quantum-dot amplifiers," IEEE J. Sel. Top. Quantum Electron. **6**, 544-551 (2000).
6. P. Borri, S. Schneider, W. Langbein, U. Woggon, A. E. Zhukov, V. M. Ustinov, N. N. Ledentsov, Z. I. Alferov, D. Ouyang, and D. Bimberg, "Ultrafast carrier dynamics and dephasing in InAs quantum-dot amplifiers emitting near 1.3-um-wavelength at room temperature," Appl. Phys. Lett. **79**, 2633-2635 (2001)
7. M. van der Poel, E. Gehrig, O. Hess, D. Birkedal, and J. M. Hvam, "Ultrafast gain dynamics in quantum-dot amplifiers: Theoretical analysis and experimental investigations," IEEE J. Quantum Elect. **41**, 1115-1123 (2005).

#73027 - $15.00 USD
Received 21 July 2006; revised 3 October 2006; accepted 5 October 2006

8. J. Meier, M. Mojahedi, J. S. Aitchison, R. H. Wang, T. J. Rotter, C. Yang, A. Stintz, K. J. Malloy, "Gain recovery dynamics in InAs-quantum dash optical amplifiers operating at 1550nm," in *Conference on Lasers and Electro-Optics/Quantum Electronics and Laser Science Conference and Photonic Applications Systems Technologies 2006 Technical Digest (Optical Society of America, Washington, DC, 2006)*, CThGG4.
9. M. van der Poel, J. Mork, A. Somers, A. Forchel, J. P. Reithmaier, and G. Eisenstein, "Ultrafast gain and index dynamics of quantum dash structures emitting at 1.55µm," Appl. Phys. Lett. **89**, 081102-1-3 (2006).
10. J. P. Reithmaier, A. Somers, S. Deubert, R. Schwertberger, W. Kaiser, A. Forchel, M. Calligaro, P. Resneau, O. Parillaud, S. Bansropun, M. Krakowski, R. Alizon, D. Hadass, A. Bilenca, H. Dery, V. Mikhelashvili, G. Eisenstein, M. Gioannini, I. Montrosset, T. W. Berg, M. van der Poel, J. Mork, and B. Tromborg, "InP based lasers and optical amplifiers with wire-/dot-like active regions," J. Phys. D Appl. Phys. **38**, 2088-2102 (2005).
11. K. L. Hall, Y. Lai, E. P. Ippen, G. Eisenstein, and U. Koren, "Femtosecond Gain Dynamics and Saturation Behavior in InGaAsP Multiple Quantum-Well Optical Amplifiers," Appl. Phys. Lett. **57**, 2888-2890 (1990).
12. S. Weiss, J. M. Wiesenfeld, D. S. Chemla, G. Raybon, G. Sucha, M. Wegener, G. Eisenstein, C. A. Burrus, A. G. Dentai, U. Koren, B. I. Miller, H. Temkin, R. A. Logan, and T. Tanbunek, "Carrier Capture Times in 1.5 um Multiple Quantum-Well Optical Amplifiers," Appl. Phys. Lett. **60**, 9-11 (1992).
13. T. W. Berg, S. Bischoff, I. Magnusdottir, and J. Mork, "Ultrafast gain recovery and modulation limitations in self-assembled quantum-dot devices," IEEE Photonic Technol. Lett. **13**, 541-543 (2001).
14. C. N. Allen, P. J. Poole, P. Barrios, P. Marshall, G. Pakulski, S. Raymond, and S. Fafard, "External cavity quantum dot tunable laser through 1.55 µm," Physica E **26**, 372-376 (2005).
15. E. W. Bogaart, R. Notzel, Q. Gong, J. E. M. Haverkort, and J. H. Wolter, "Ultrafast carrier capture at room temperature in InAs/InP quantum dots emitting in the 1.55 mu m wavelength region," Appl. Phys. Lett. **86**, 173109-1-3 (2005).
16. H. Ju, J. M. Vazquez, Z. Li, R. Notzel, T. de Vries, D. Lenstra, Q. Gong, P. J. van Veldhoven, J. H. Wolter, G. D. Khoe, and H. J. S. Dorren, "Polarization-dependent carrier dynamics in a passive InAs/InP quantum dot waveguide," Opt. Commun. **259**, 861-867 (2006).
17. K. L. Hall, G. Lenz, A. M. Darwish, and E. P. Ippen, "Subpicosecond Gain and Index Nonlinearities in InGaAsP Diode-Lasers," Opt. Commun. **111**, 589-612 (1994).
18. A. J. Zilkie, J. Meier, P. W. E. Smith, M. Mojahedi, J. S. Aitchison, P. J. Poole, C. N. Allen, P. Barrios, and D. Poitras, "Characterization of the ultrafast carrier dynamics of an InAs/InGaAsP quantum dot semiconductor optical amplifier operating at 1.55 µm," in *Photonic Applications in Nonlinear Optics, Nanophotonics, and Microwave Photonics*, R. A. Morandotti, H. E. Ruda, J. Yao, eds., Proc. SPIE **5971**, 91-100 (2005).
19. J. Mork, T. W. Berg, M. L. Nielsen, and A. V. Uskov, "The role of fast carrier dynamics in SOA based devices," IEICE Trans. Electron. **E87C**, 1126-1133 (2004).
20. C. K. Sun, H. K. Choi, C. A. Wang, and J. G. Fujimoto, "Femtosecond Gain Dynamics in InGaAs/AlGaAs Strained-Layer Single-Quantum-Well Diode-Lasers," Appl. Phys. Lett. **63**, 96-98 (1993).

1. Introduction

Self-assembled quantum dot (QD) semiconductor optical amplifiers (SOAs) have recently attracted attention for integrated high-bit-rate (>40 Gb/s) signal processing because their carrier recovery times have been shown in some cases to be 10 to 100 times faster than quantum-well or bulk amplifier devices [1-4]. Assessing the speed performance of a QD SOA however requires a detailed understanding of its ultrafast dynamics. QD SOAs in ultrafast dynamics studies to date [5-7] have been based on the InAs/AlGaAs and InAs/InGaAs material systems, operating in the 1.1 µm to 1.3 µm wavelength range. The gain dynamics of these quantum dot structures were shown to have recovery times of less than 10 ps. The ultrafast dynamics of InAs/InGaAlAs/InP quantum dash (QDASH) SOAs at 1.55 µm have recently been reported [8-10], and the dynamics of multiple quantum well (MQW) SOAs at 1.55 µm have also been well characterized [11,12]. These QDASH and MQW devices were found to typically have recovery times of ~100 ps or larger. The >10x faster gain recoveries measured in QDs thus suggest superior speed performance, which has clearly been demonstrated in [1], however debate remains as to the nature of the long-lived gain recoveries in QDs and whether this superior performance would endure at high repetition rates of 40 Gb/s or greater [9,13]. Recently, QD lasers based on InAs/InGaAsP/InP have been demonstrated to operate at 1.55 µm [14]. The ultrafast dynamics of these QDs have been reported in unprocessed wafers and passive waveguides [15,16], but to date have not been studied in active structures processed into their final amplifier form. In this work we

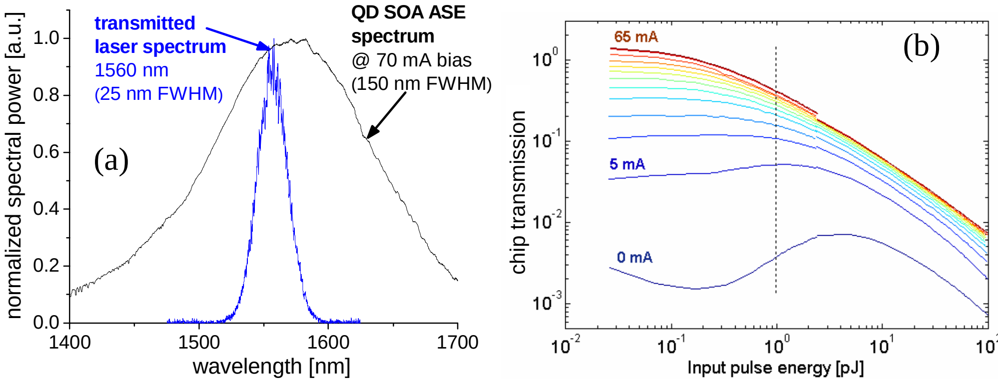

Fig. 1. (a). ASE spectrum of the QD SOA under 70mA bias, overlayed with the spectrum of the OPO pulses transmitted through the SOA in the transparent TM polarization state. (b) Device transmission versus input pulse energy under bias currents from 0 to 65 mA in increments of 5 mA. The dashed vertical line shows the pump pulse energy used in the pump-probe experiments. Two separate measurements were needed to achieve the full 40 dB range of input energies, resulting in the small break in the curves at ~2 pJ.

report the first heterodyne pump-probe characterization of the amplitude and phase dynamics of an InAs/InGaAsP/InP QD SOA at its near-1.55 μm gain peak.

2. Sample and experiment

The SOA sample measured was an AR-coated QD laser from those reported in [14]. The p-i-n doped ridge-waveguide diode was grown by chemical beam epitaxy on an exactly oriented (100) InP substrate. The 400-nm-thick active region contained five stacked layers of self-assembled (Stranski-Krastanov) InAs QDs embedded in InGaAsP, with a $1.5\times10^{10}\,\mathrm{cm}^{-2}$ planar dot density, and a quaternary composition of $In_{0.816}Ga_{0.184}As_{0.392}P_{0.608}$ which provides a 0.22 eV energy barrier for carrier escape from the QDs. The final devices were 1 mm in length. Figure 1(a) shows the amplified spontaneous emission (ASE) spectrum measured for the SOA, peaking at ~1575 nm. The ASE bandwidth is a result of inhomogeneous broadening due to the size distribution of the QDs. Figure 1(b) shows the chip transmission of the amplifier versus input pulse energy, with a 33% coupling efficiency, for bias currents between 0 and 65 mA. The curves show gain and absorption bleaching for input pulse energies below ~5 pJ, and a linear decrease in transmission above ~5 pJ due to two-photon absorption. With 65-mA bias current, the maximum device gain is 0.2 dB (0.87 dB/cm).

The pump-probe experiments were performed using a Ti:Sapphire pumped optical parametric oscillator (OPO), providing nearly Fourier-limited 150 fs pulses at a repetition rate of 76 MHz. Figure 1(a) also shows the spectrum of the OPO laser pulses, overlaid with the QD amplifier ASE spectrum. The OPO wavelength was set to 1560 nm, near the peak of the ASE spectrum, and was TE-polarized for the pump-probe measurements, so as to characterize the resonant gain of the QD ensemble. The three-beam degenerate heterodyne pump-probe setup [6,17] used for the measurements is shown schematically in Fig. 2. The OPO light is split into three beams, pump, probe and reference. The pump beam passes through a motorized delay stage, to control the time delay, Δt, between the pump and probe pulses. Acousto-optic modulators (AOMs) upshift the frequency of the probe and reference beams by 53.5 MHz and 52 MHz, respectively. The three beams are then recombined at the input to the device under test (DUT) such that the reference pulses lead the probe pulses by a fixed delay of ~4.5 ns. An RF lock-in amplifier detects the amplitude and phase of the 1.5 MHz beat signal from a Michelson interferometer at the output of the DUT. The reference pulses pass through the sample before the pump pulses in all cases, and therefore remain unchanged.

Consequently, the probe-reference beat signal gives the changes in probe amplitude and phase due to changes in the absorption/gain and refractive index induced in the SOA by the

#73027 - $15.00 USD
Received 21 July 2006; revised 3 October 2006; accepted 5 October 2006

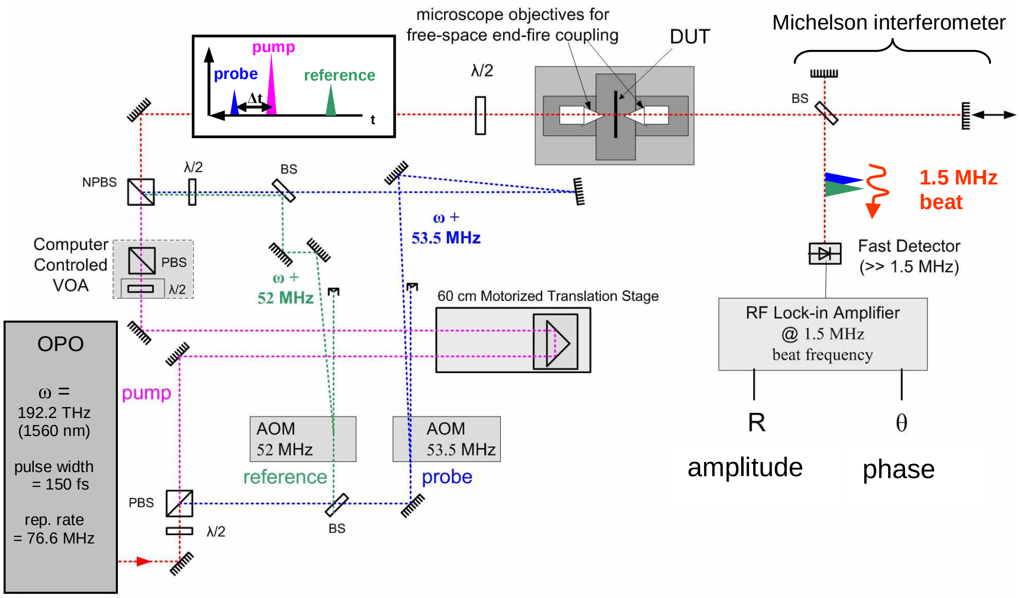

Fig. 2. Schematic of our heterodyne pump-probe experiment. OPO = optical parametric oscillator, λ/2 = half-wave plate, PBS = polarization beam-splitting cube, BS = beam splitter, AOM = acousto-optic modulator, NPBS = non-polarizing beam-splitting cube, VOA = variableoptical attenuator, DUT = device under test. Δt is pump-probe delay.

pump pulses. A more detailed description of the setup is given in [18]. The pulse energies of the pump and probe were 1 pJ and 0.09 pJ, respectively, and the pulse energy of the reference was set to equal that of the probe. Referring to Fig. 1(b), a 1 pJ input pump pulse energy is in the absorption/gain saturation regime, so as to induce carrier population changes, while the 0.09 pJ probe energy is in the small-signal regime.

3. Experiment results and discussion

3.1 Amplitude Dynamics

Figure 3(a) shows the ultrafast pump-induced amplitude dynamics measured in our QD SOA, for increasing bias currents, together with exponential fits to the data (dotted lines). The transparency current was approximately 40 mA, where the step in transmission due to changes in carrier density is zero. For currents below 40 mA, the amplifier is in the absorption regime, and for currents above, in the gain regime. At zero pump-probe delay, there is an instantaneous transmission decrease which we attribute to two-photon absorption (TPA) (plus any additional coherent artifact [17]), since the magnitude is weakly dependant on bias current, and the shape closely matches the autocorrelation trace of the laser pulses. Following this, the ultrafast transmission increase and subsequent negative dynamic with 1.5 ps recovery matches carrier heating (CH) and spectral hole burning (SHB) [5,17,19]. The CH dynamic is due to a combination of two pump-pulse-induced processes, stimulated absorption (or stimulated emission) heating, and free carrier absorption (FCA) heating, which transiently heat the carrier distributions by creating 'hot' carriers above the average carrier energy (or by removing 'cold' carriers below the average energy in the stimulated emission case). The hot carriers then cool back to the lattice temperature through phonon-assisted carrier-carrier scattering. The SHB dynamic is due to intradot carrier-carrier scattering which replenishes (gain regime) or empties (absorption regime) the dot ground state after the spectral hole is burned by the pump. Good exponential fits to the traces were achieved by fitting the data to an impulse response function given by $h(t) = h_{TPA} + h_{cr} + h_{CH} + 1$, convolved with the autocorrelation trace of the laser pulse [17]. Here $h_{TPA} = a_{TPA} u(t)\delta(t)$ models the instantaneous

Received 21 July 2006; revised 3 October 2006; accepted 5 October 2006

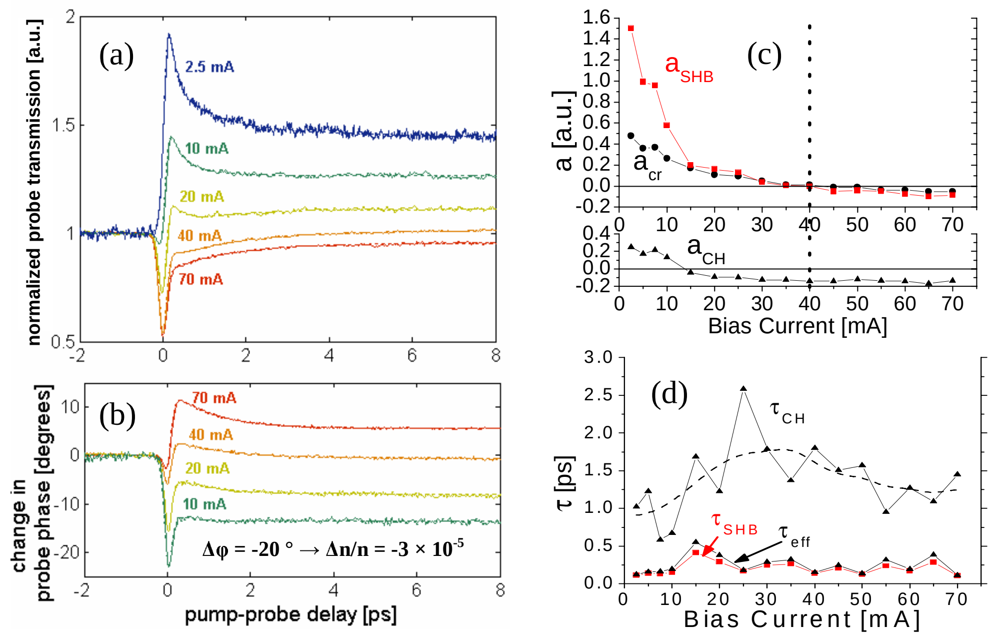

Fig. 3. Measured change in probe amplitude (a) and phase (b) versus pump-probe delay for bias currents up to 70 mA. The dotted lines show the fits to the traces using Eq. (1). (c) Magnitudes of the SHB (red squares), carrier density step (black circles), and CH (black triangles) fit components from the fits in (a), vs. bias current. (d) Corresponding 1/e lifetimes, with dashed line showing smoothed trend in τ_{CH}.

(delta-function) TPA response, $h_{cr} = a_{cr}u(t)$ the step response due to the long-lived carrier density change, and h_{CH} accounts for the carrier heating and carrier cooling dynamics, and is in the 'delayed carrier heating' form for the carrier heating component as in [17]:

$$h_{CH} = u(t)\{a_{CH}\exp(-t/\tau_{CH})[1-\exp(-t/\tau_{eff})] + a_{SHB}\exp(-t/\tau_{SHB})\}. \qquad (1)$$

In these equations, *u(t)* is the unit step function, the *a* coefficients are the magnitudes of the exponential terms used in the fitting, the τ constants are the 1/*e* decay times, and $1/\tau_{eff} = 1/\tau_{SHB} - 1/\tau_{CH}$. Figures 3(c) and 3(d) show the trends of the *a* and τ values versus bias current found from the fitting. We obtained $\tau_{eff} \approx$ 0.2-0.3 ps, which represents the delay in the transfer of excess carrier energy to the surrounding carrier distribution (i.e. carrier heating time), and $\tau_{CH} \approx$ 1.5 ps, which is the carrier heating recovery time (i.e. carrier cooling time). a_{SHB} crosses zero at transparency and closely follows the magnitude of the step carrier density change a_{cr} with increasing bias current [Fig. 3(c)], and $\tau_{SHB} \approx$ 0.2-0.25 ps, consistent with spectral hole refilling via intradot phonon-assisted carrier-carrier scattering [7].

The trends in a_{CH} and τ_{CH} suggest that the carrier heating is caused by a combination of free carrier absorption (FCA) and stimulated transition processes. The CH and SHB impulse response model and fitted lifetimes (particularly at high bias currents) match closely to those reported for the InGaAs/InGaAsP quantum well SOA in [17]. Looking at the trend in a_{CH} in Fig. 3(c), for currents above 10 mA we observe a negative a_{CH}, increasing in magnitude as the bias current, and thus the population of free carriers, is increased. We thus suggest that the carrier heating is dominated by free carrier absorption (FCA) in our QDs at high bias currents, as in the quantum well. FCA-dominated heating is in contrast to the CH responses seen in previous studies of 1.1 and 1.3 μm QDs [5], which attributed weaker CH dynamics to a lack of FCA. In addition, however, for currents below 10 mA in our dots, we observe a *positive* a_{CH} term, implying pump-induced *carrier cooling* is occurring. This cooling must be due to stimulated transition processes, since FCA processes always lead to a heating of the distribution. In this case stimulated absorption cools the carrier distribution by adding cool carriers below the average energy, and are dominant over a weaker FCA heating because of the lower carrier density. FCA heating still dominates at high currents, however, since stimulated transitions go to zero at transparency, and are still relatively weak for higher currents because of the low device gain. To our knowledge carrier cooling has been only observed once previously in measurements on an InGaAs/AlGaAs QW amplifier [20]. The trend in $\tau_{CH,}$ shown by the dashed line in Fig. 3(d) also supports this model for carrier heating in our dots, and is in agreement with [20]. At currents of 10 mA and below, τ_{CH} approaches a value of ~0.8 ps, corresponding to the stimulated transition heating lifetime; at currents near transparency, τ_{CH} approaches an FCA heating value of ~1.5 ps; and at currents above transparency, τ_{CH} drops slightly from 1.5 ps as the effects of stimulated transition heating again begin to increase as the gain increases.

3.2 Phase Dynamics

Figure 3(b) shows the ultrafast phase dynamics and exponential fits, measured simultaneously with the amplitude dynamics. The changes in phase are proportional to changes in refractive index in the SOA, the -20° Kerr-effect change at zero delay corresponding to $\Delta n/n = -3 \times 10^{-5}$. The phase responses show an exponential decay following the instantaneous Kerr dynamic, which fitted well with a single exponential with a 1-1.5 ps lifetime for all bias currents, consistent with the amplitude CH recovery times in Fig. 3(a). There is an absence of an SHB dynamic in the phase responses, which is expected for hole burning that is symmetric about the center frequency [5,17]. The large, always positive, CH dynamics observed in the phase traces at high bias currents corroborate strong FCA-induced carrier heating.

3.3 Long-lived carrier recovery dynamics

The long-lived carrier recovery times are also important since they dictate the ultrafast switching rate. Figure 4 shows the changes in transmission measured over 2 ns in our QD SOA, along with single-exponential fits to the data (dotted lines). In the absorption regime [Fig. 4(a)], we measured a 400 ps recovery time, which represents the electron-hole pair (exciton) decay time, either through spontaneous radiative recombination, or through carrier escape from the dots. In the gain regime [Fig. 4(b)] we measured a much shorter recovery time of 15 ps, promising for >40 GHz ultrafast signal processing. In the gain regime, the gain saturation recovers when the carrier population is replenished via relaxations from excited

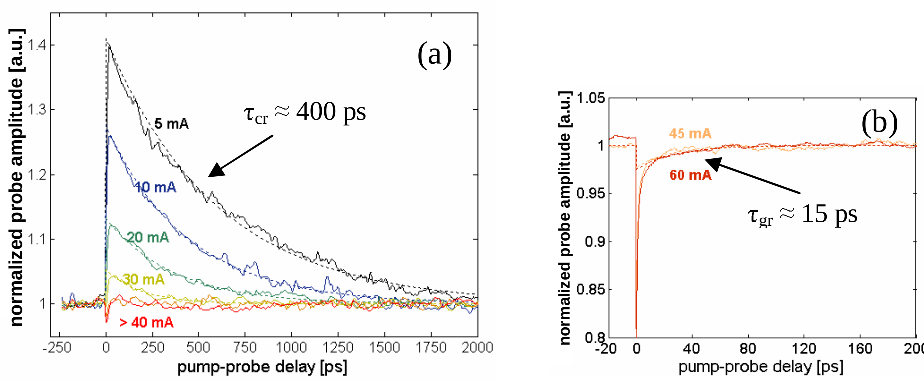

Fig. 4. Probe transmission versus pump-probe delay over 2 ns showing the long-lived carrier dynamics. Dotted lines show the single-term exponential fits to the data. (a) shows the dynamics for 5-30 mA bias currents (absorption regime), and (b) shows a zoom of the dynamics at 45 and 60 mA (gain regime), illuminating the short 15 ps gain recovery time.

states. In agreement with studies performed on highly-confined InAs/AlGaAs and InAs/InGaAs 1.3 μm QD SOAs [6,7], we attribute the fast 15 ps gain recovery to phonon-mediated carrier capture into the dots, and the slow 400 ps absorption recovery to a slow spontaneous carrier recombination time. The long 400 ps absorption decay time is expected for highly-confined dots, since the high potential barrier to the wetting layer states suppresses carrier escape processes. Also, for the InAs/InGaAs 1.1 μm QD SOA with less confined dots in [5], a much shorter few-hundred femtosecond gain recovery time dictated by intra-dot Auger scattering was found, further supporting that high quantum confinement has been achieved in our dots, and suggesting that reducing the confinement in our dots may shorten the gain recovery time into the sub-picosecond regime.

4. Conclusion

In summary, we have reported the first characterization of the ultrafast gain and refractive index dynamics of an InAs/InGaAsP-based QD SOA operating in the 1.55 μm wavelength range. A 15 ps gain recovery time was found, limited by the dot carrier capture time, similar to the gain recoveries in InAs/InGaAs 1.3 μm QD SOAs. The gain recovery time may be shortened further by reducing the wetting layer-QD energy difference. Strong CH dynamics were found, in contrast to previous 1.3 μm dots, and more similar to InGaAs/InGaAsP quantum well SOAs. We also found FCA-dominated carrier heating at high bias currents, and stimulated-transition-dominated heating resulting in carrier cooling at low bias currents, unlike the CH dynamics observed in any previous QD SOAs. The 15 ps gain recovery makes this device capable of near 100 GHz switching speeds at 1.55 μm.

Acknowledgments

The author gratefully acknowledges helpful discussions with D. C. Hutchings and M. Y. Xu. This work was supported by NSERC, CFI, CIPI, and AAPN research grants, an Ontario Graduate Scholarship, and an Edward S. Rogers Sr. Graduate Scholarship.